Polymer Solar Cells Using Single-Wall Carbon Nanotubes Modified with Thiophene Pedant Groups

ARTICLE *in* THE JOURNAL OF PHYSICAL CHEMISTRY C · NOVEMBER 2007

Impact Factor: 4.77 · DOI: 10.1021/jp074979n

Polymer Solar Cells Using Single-Wall Carbon Nanotubes Modified with Thiophene Pedant Groups

Ana Flávia Nogueira,* Bruno S. Lomba, Mauro A. Soto-Oviedo, and Carlos Roque Duarte Correia

Laboratório de Nanotecnologia e Energia Solar, LNES, Instituto de Química, UNICAMP, C. Postal 6154, 13084-971, Campinas SP, Brazil

Paola Corio

Instituto de Química, Universidade de São Paulo, C. P. 26077, 05513-970, São Paulo SP, Brazil

Clascídia A. Furtado

Laboratório de Química de Nanoestruturas, Centro de Desenvolvimento da Tecnologia Nuclear, CDTN/CNEN, C. P. 941, 31123-970, Belo Horizonte, MG, Brazil

Ivo A. Hümmelgen

Departamento de Física, Universidade Federal do Paraná, UFPR, C. P. 19044, 81531-990, Curitiba PR, Brazil

Received: June 26, 2007; In Final Form: August 21, 2007

Single-wall carbon nanotubes (SWCNT) have attracted great interest for applications in a variety of research areas, including electronics and functional materials. However, a good dispersion of these materials in polymer matrices is a demanding factor in order to obtain more homogeneous and less bundled films for constructing optoelectronic and electrochemical devices. In this report we describe a covalent modification with thiophene groups located at the edges and at defects in SWCNT to modify the interaction with the polymer matrix aiming at its application in solar cells. The modified SWCNT and its composites with poly(3-octylthiophene) were characterized by Raman, infrared, UV−vis, and luminescence spectroscopies and cyclic voltammetry. The best bulk heterojunction solar cell was obtained using 5 wt % of the modified carbon nanotube (SWCNT-THIOP) and shows open circuit voltage (VOC), short-circuit current (I_{sc}), and efficiency (η) of 0.75 V, 9.5 μA cm^{-2}, 0.184%, respectively.

Introduction

Carbon nanotubes (CNT), in particular, single-wall carbon nanotubes (SWCNT), are attracting much attention in the scientific community because of their remarkable properties, such as electrical, optical, and thermal properties, mechanical strength, and high catalytic surface area.[1−3] In addition, CNT can be chemically modified, covalently or noncovalently, allowing a good dispersion in a polymer matrix. Such modifications give rise to high performance polymer nanocomposites at low loadings of CNT.[4]

SWCNT are one-dimensional nanowires that can be found in metallic and semiconducting states. They can readily accept electrons and transport them under nearly ideal conditions along the axis.[5]

Organic photovoltaic solar cells are of great interest as a potential source of renewable energy and as a promising alternative to inorganic solar cells. These cells are constructed from inexpensive organic materials, employ easy preparation and deposition methods, and can be fabricated on a large scale using flexible substrates. The introduction of the bulk heterojunction concept,[6−7] where the donor and acceptor organic materials are blended in a nanoscale morphology, allows production of organic solar cells with efficiencies higher than 4%.[8] The acceptor molecules usually employed in these cells are fullerene derivatives, particularly 1-(3-methoxycarbonyl)-propyl-1-phenyl-(6,6)C_{61}, known as PCBM. In these cells the excitons photogenerated in the organic semiconductor (usually a conducting polymer) are dissociated at the interface with the fullerene molecule because of different electron affinities and ionization potentials. After dissociation, the charges are collected in the appropriate electrodes under the influence of a built-in electrical field, normally generated by the difference in the electrode workfunction.[9] Organic solar cells using fullerenes as acceptor materials require a high content of these molecules in order to achieve a percolation path for efficient electron transport. Usually, organic solar cells are constructed with a polymer:fullerene ratio of 1:4.[9] The use of carbon nanotubes in this type of device is a particularly attractive approach for several reasons. The extremely high surface area offers an ideal morphological architecture for exciton dissociation. Their high aspect ratio ($>10^3$) allows the establishment of percolation pathways at low doping levels, providing the means for high carrier mobility and efficient charge transfer to the appropriate electrodes. Conducting polymer nanocomposites have been developed with extremely low percolation thresholds. For

* To whom correspondence should be addressed. Phone: + 55-19-3521-3029. Fax: +55-19-3521-3023. E-mail: anaflavia@iqm.unicamp.br.

10.1021/jp074979n CCC: $37.00
Published on Web 11/20/2007 PAGE EST: 8

SWCNT-epoxy composites, electrical conductivity has increased by at least 10^7 between 0.1 and 0.2% w/w loading.[10,11]

Ago and co-workers were the first to explore the electronic properties of a composite of multiwall carbon nanotubes (MWCNT) and a conducting polymer.[12] They reported that a strong interaction in the excited-state occurs in the composite, indicating energy transfer between the conducting polymer and the MWCNT. Since their pioneering investigation, several groups have exploited SWCNT to improve carrier generation and collection efficiency in bulk heterojunction[13−17] and photoelectrochemical cells.[18]

In the first report of a polymer solar cell using SWCNT as acceptor material, Kymakis and co-workers demonstrated that by blending poly(3-octylthiophene) (P3OT) with only 1 wt % of SWCNT, the device performance increases with respect to both open circuit voltage (V_{oc}) and short-circuit current (I_{sc}). This photovoltaic effect can be ascribed to the introduction of internal polymer/nanotube junctions within the polymer matrix. These junctions allow excitons to be dissociated and also create a continuous path for electron transport to the charge-collecting electrode.[19,20] More recently this group demonstrated that the annealing process can be a favorable approach to improve film morphology and as a consequence device efficiency.[21] Photoelectrochemical cells using carbon nanotubes were also assembled by Kamat and co-workers.[18,22] The authors confirmed the p-type character of the semiconducting SWCNT and also its ability to promote both charge separation and electron transport. Different carbon nanotube structures such as multiwall and double wall, as well as SWCNT sensitized with pyrene molecules, had their photoelectrochemical properties investigated by Guldi and co-workers.[23] According to the authors, thin MWCNT are the most promising material for energy conversion. In more recent work, Castrucci et al. confirmed those expectations, demonstrating that, in fact, MWCNT are much more effective than SWCNT in photocurrent generation.[24]

Several groups have also carried out an extensive investigation on the excited charge-transfer properties between hybrids of SWCNT and organic semiconductors by means of transient absorption techniques.[25−31] The favorable energy levels and high electron affinity of SWCNT result in the creation of long-lived radical ion-pairs after excitation of the organic semiconductor chromophore.

Transparent and highly conducting carbon nanotube networks are also very attractive to be used as hole-collecting electrodes in organic light-emitting diodes and organic solar cells.[32−34] The substitution of indium-tin oxide film (ITO) electrodes by single-wall carbon nanotubes is advantageous,[35] especially considering the high increase in indium prices observed recently, achieving the highest level of the last decades.[36] Adjusting the carbon nanotube electrodes' work function by chemical modification is another area that can be exploited, allowing application of these materials in both collecting electrodes and substantially reducing the device production costs.

However, all SWCNT organic solar cells reported until now have a common characteristic of low ISC and fill factors (FF). These are important factors that impose power conversion efficiency (η) limitations. The low efficiencies observed by the SWCNT-based solar cells can be derived from several factors: presence of metallic SWCNT that short-circuit the devices (reducing the shunt resistance), impurities (mainly catalyst particles), problems with SWCNT aggregation, and low charge carrier mobility in the polymer matrix.

In this work we report the fabrication and characterization of bulk heterojunction solar cells using a chemically modified single-wall carbon nanotube and P3OT. Recently, we demonstrated that this modified carbon nanotube combined with a polarized polybithiophene layer improved the solar cell open circuit voltage to 1.8 V, giving a conversion efficiency of 1.5%.[37] The purpose of chemically modifying the SWCNT with 2-(2-thienyl)ethanol was to introduce pendant thiophene groups in order to promote a better dispersion of these materials in the polymer matrix of polythiophene. It is well-known that a homogeneous distribution of SWCNT in the polymer is difficult to achieve. In general, carbon nanotube bundles remain in the polymer, attracted to each other by van der Waals interactions. Thus, the presence of thiophene groups mainly located at the edges and defects of the carbon nanotubes can promote an improvement in SWCNT dispersion and compatibility with the conducting polymer employed and can result in more efficient polymer/nanotube solar cells because of reduced phase segregation.

TABLE 1: Electrical Parameters Obtained from the *I*−*V* Curves under Simulated AM 1.5 Illumination (Φ = 10.6 W m^{-2}) for the P3OT + SWCNT-THIOP Solar Cells at Different Carbon Nanotube Doping Levels and for the P3OT + SWCNT Solar Cell

	V_{oc} (V)	I_{sc} (μA cm^{-2})	η(%)
P3OT + 5 wt % SWCNT	0.19	7.0	0.036
P3OT + 1 wt % SWCNT- THIOP	0.24	3.8	0.019
P3OT + 3 wt % SWCNT- THIOP	0.36	7.3	0.062
P3OT + 5 wt % SWCNT- THIOP	0.75	9.5	0.184
P3OT + 7 wt % SWCNT- THIOP	0.48	7.9	0.085

Experimental Section

Materials. All solvents and chemicals were reagent-grade quality, obtained commercially, and used without further purification. P3OT was chemically synthesized following a procedure reported elsewhere.[38] Carbon nanotube soot, produced by the arc-discharge method using ~4 atomic % Ni−Y loaded carbon electrodes, was obtained from Carbolex, Inc. The samples were first purified by dry oxidation at 350 °C in air for 1 h to remove amorphous carbon, followed by reflux in HNO_3 (3 mol L^{-1}) for 8 h, to remove metallic particles remaining from the synthetic procedure. The amount of SWCNT and residual metallic particles were estimated by thermogravimetric analysis to be 70 (at least) and 10 wt %, respectively. The purification protocol used here is known to add carboxylic groups to the nanotube edges and defects. These materials will be referred as SWCNT-COOH.[39]

Chemical Modification of SWCNT. The introduction of the pendant thiophene groups was accomplished, starting from the SWCNT-COOH. The synthetic route was the same employed by Langa and co-workers to produce soluble SWCNT-containing *n*-pentyl esters.[40] Thus, 15 mg of SWCNT-COOH and 3 mL of thionyl chloride (Aldrich) were mixed and stirred at 80 °C for 24 h. The crude reaction mixture was then evaporated in vacuum to remove the excess of $SOCl_2$, followed by addition of 2 mL of 2-(2-thienyl)ethanol (Aldrich). The resulting solution was stirred for 72 h at 80 °C. The product (named as SWCNT-THIOP) was washed with water to remove the excess of thiophene and dried in vacuum. The complete chemical route containing all the modification steps is displayed in Scheme 1.

Preparation and Characterization of the SWCNT Materials. Pristine SWCNT, SWCNT-COOH and SWCNT-THIOP were characterized by Raman and infrared spectroscopies. Infrared spectra in the 600 − 4000 cm^{-1} wavenumber range of the pristine SWNT-COOH and SWCNT-THIOP were collected in the transmission mode of a Centaurus microscope (magni-

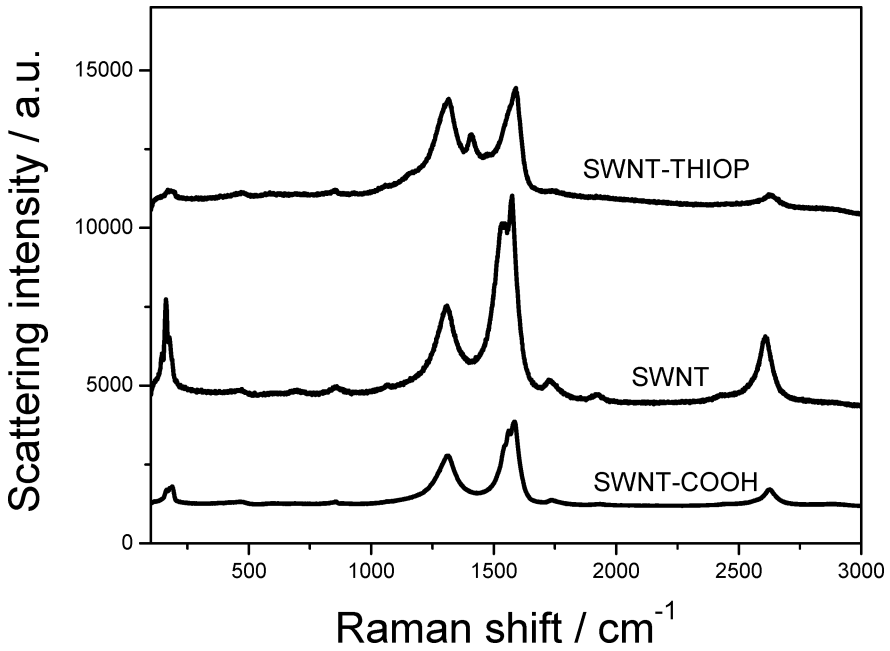

Figure 1. Resonance Raman spectra of the carbon nanotube materials: SWCNT, SWCNT-COOH, and SWCNT-THIOP. E_{laser} = 1.96 eV (632.8 nm).

fication 10×, observed region 150 × 150 μm^2) attached to a FTIR Nicolet (Nexus 470) spectrometer. The spectral resolution was better than 4 cm^{-1}, and the spectra were averaged over 64 scans. Details of sample preparation for FTIR measurements can be obtained elsewhere.[41] The Raman spectra were obtained using a Renishaw Raman System 3000 equipped with a CCD detector and an Olympus microscope (BTH2). The laser was focused on the sample by a ×50 lens. The experiments were performed at ambient conditions using a back-scattering geometry. The samples were irradiated with the 632.8 nm line of a He−Ne laser (Spectra Physics). The AFM images were acquired in-air using an AutoProbe CP (Thermo Microscopes) operating in noncontact mode.

Composites of P3OT with SWCNT, SWCNT-COOH, or SWCNT-THIOP were prepared by adding P3OT to a SWCNT dispersion in toluene (ultrasonicated for 2 h) so that the final concentration of the polymer was 10 mg mL^{-1}. The system was then stirred for 24 h prior deposition. For the SWCNT modified with thiophene groups, the content of the SWCNT-THIOP was varied from 1 to 7 wt % in the composite with P3OT by selecting appropriate proportions of both dispersions. The SWCNT composites with P3OT were characterized by UV−vis and luminescence spectroscopies and by cyclic voltammetry. UV−vis spectra were measured with a HP 8453 spectrophotometer and fluorescence spectra with a ISS Photon Counting Spectrofluorometer. Cyclic voltammetry was carried out in a conventional three electrode-cell using an Eco Chemie Autolab PGSTAT 10 unit. As reference electrode we used Ag/AgCl, and the electrolyte was 0.1 mol L^{-1} $(CH_3)_4NBF_4$.

Solar Cell Assembly and Characterization. The bulk heterojunction devices were prepared by spin-coating 10 mg mL^{-1} of the SWCNT + P3OT or SWCNT-THIOP + P3OT suspensions in toluene on the top of an ITO covered glass (Delta Technologies, Inc), previously spin-coated with PEDOT:PSS solution (Bayer). In the sequence, the aluminum top metal contact was evaporated at 10^{-6} Torr. Layer thickness was estimated using a Dektak3 surface profiler. Device performance characterization was carried out by measuring the current vs voltage ($I(V)$) characteristics in the dark and under AM 1.5 spectral distribution, which was obtained using a 150 W Oriel solar simulator plus filters. The samples were illuminated through the glass substrate, and the radiance was controlled using neutral filters. The radiance was determined using a calibrated silicon photodetector.

Results and Discussion

Spectroscopy and Electrochemical Characterization of the SWCNT Materials and Their Composites with P3OT. Since Raman spectroscopy is sensitive to both electronic and vibrational structures of the carbon nanotubes, the technique can be used to probe the modification of their electronic and vibrational properties caused by the introduction of different anchoring groups. The Raman spectra of the SWNT (before purification), SWNT-COOH and SWNT-THIOP are shown in Figure 1. For the nonpurified SWNT, at least four distinct tube radii exist in the CarboLex material when excited with 632.8 nm radiation. The main peak for the radial breathing mode (RBM) occurs at ∼162 cm^{-1}. This corresponds to a tube diameter of 1.4 nm.[42] Other less intense peaks appear at ∼144, 176, and 186 cm^{-1}. The introduction of carboxylic and thiophene groups is expected to change the force constant of the RBM mode, and as a consequence this band was reduced in intensity and shifted to higher energy values.[39] This upshift is difficult to quantify given the low frequency and the weak nature of the RBM after the chemical treatment. Only two weak peaks were observed at ∼163 and 187 cm^{-1} after both purification (SWNT-COOH) and functionalization (SWNT-THIOP) processes.

Since the frequency mode is related to the square root of the change in an effective force constant, the high-frequency modes are expected to upshift much more than the RBM.[39] The D-band around 1308 cm^{-1} for the SWNT sample is assigned to a structural disorder of the carbon nanotubes, which involves the presence of amorphous carbon and defects in the graphitic layer. The strong band in the frequency range 1540 − 1650 cm^{-1} is associated with the $\nu_{(C-C)}$ stretching modes (tangential G-band). The line shape of the tangential feature is associated to the semiconducting and metallic electronic structures of carbon nanotubes.[43] Here, the G-band profile for the pristine SWNT shows a higher-frequency component (at *ca.* 1573 cm^{-1}) and a

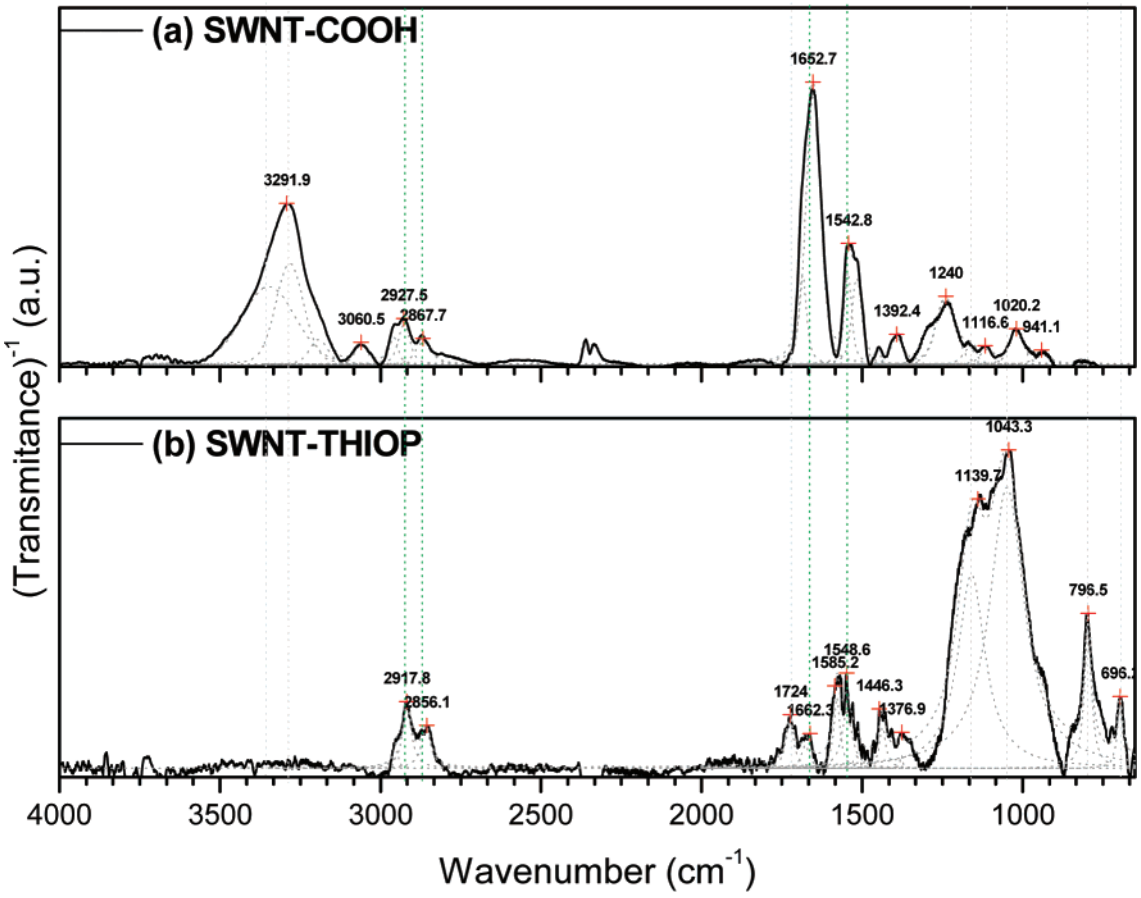

Figure 2. Infrared spectra of the carbon nanotube materials (a) SWCNT-COOH and (b) SWCNT-THIOP.

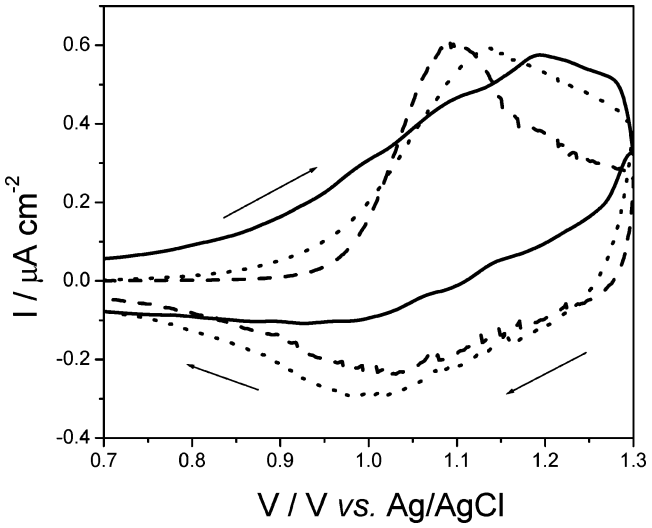

Figure 3. Cyclic voltammetry of the pristine P3OT film and its composites with single-wall carbon nanotubes deposited over ITO electrodes: P3OT (full line); P3OT + 5 wt % of SWCNT-COOH (dotted line); P3OT + 5 wt % of SWCNT-THIOP (dashed line). A 0.1 mol L^{-1} concentration of $(CH_3)_4NBF_4$ in acetonitrile as supporting electrolyte. Scan rate of 30 mV s^{-1}.

lower-frequency component (at *ca.* 1540 cm^{-1}) with a Breit−Wigner−Fano (BWF) line shape. These features are attributable to the presence of metallic SWNT in the sample used.[44] The second-order spectrum of SWNTs is dominated by the G′-band, which is the highly dispersive harmonic of the D-band, and is observed here between 2600 and 2630 cm^{-1}. This band is sensitive to the electronic density of CNT and shows a considerable displacement with chemical modification. In fact, an upshift of ∼4, 10, and 21 cm^{-1} was respectively observed for D-, G-, and G′-bands after purification. It is well-known that removing electrons from SWNT (i.e., p-doping or oxidizing) results in an upshift in the G-band peak,[45] and the concomitant upshift of the D-band and G′-band is another signal of charge transfer. After the HNO_3-based treatment, the removal of electrons from the sp^2 carbon network can occur by inductive effect. After the chemical modification with thiophene-containing groups, G- and G′-band upshifted again by 4 and 3 cm^{-1}, respectively. The peak positions are now at ∼1587 and 2632 cm^{-1} for the SWNT-THIOP sample.

The intensity ratio between the G- and D-band can be related to the degree of disorder found in the carbon nanotube materials.[46] Here, an increased intensity of the D-band with respect to the G-band when compared with the pristine SWNT can be observed after chemical treatment. We interpret this result as evidence for a decrease in structural order in the SWNT bundles after nitric acid reflux during the purification step, which breaks the $C(sp^2)-C(sp^2)$ graphitic bonds forming new $C(sp^3)$ bonds. This symmetry breaking is also responsible for the decrease in the intensity of the RBM mode of the modified SWCNT relative to pristine SWCNT, since the breathing mode is inhibited by the presence of the anchoring groups.

Even though we consider Raman scattering one of the most sensitive probes of nanotube wall damage, it is interesting to illustrate the Raman results with electron microscopy. In Figure 3S (see Supporting Information), we display the HRTEM image of our bundles of SWNTs that have been subjected to dry oxidation and nitric acid reflux and then dispersed in DMF. The image is representative of the whole sample. Whereas the Raman spectra of these purified materials show a clear difference due to wall damage, the HRTEM evidence for damage is more

subtle but nevertheless evident. Carbon fragments attach to the tube walls (see arrows in Figure 3S). Small notches form in the wall of tubes that are on the outside of the bundle. Both coating and notches may contribute to D-band scattering and a broad G-band contribution superimposed on the nanotube G-band.

The esterification reaction between the SWCNT-COOH and 2-(2-thienyl)ethanol promotes the anchoring of the thiophene groups in the carbon nanotube extremities. The observation of a band at 1410 cm^{-1}, corresponding to the symmetrical stretching Cα═Cβ of the thiophene ring of 2-(2-thienyl)ethanol in the SWNT-THIOP spectrum corroborates the success of the carbon nanotube modification. Another interesting observation regards the hyperchromic effect in the D-band of the SWNT-THIOP when comparing to that of the SWNT-COOH, indicating an increase in the degree of disorder even after the esterification reaction, and the presence of relatively more π-electrons resulting from the introduction of the thiophene ring.

The functional groups added to the SWNT ends and defects after each purification and chemical modification step were identified by infrared transmission through thin films of the nanotube samples. Infrared spectra of the SWNT-COOH and the SWNT-THIOP are presented in Figure 2a and 2b, respectively. Unambiguous assignments for those spectra are not able to be made because of the superposition of vibrational modes of the groups present in the complex surface of a chemically processed nanotube. In any case, the clear spectral changes indicate an alteration of the chemical environment from SWNT-COOH to SWNT-THIOP. For the purified sample (SWNT-COOH, Figure 2a), the presence of three functional groups was identified: phenol, quinone, and carboxylic acid. The bands at 3348, 3060, 1392, and 1239 cm^{-1} are, respectively, assigned to O−H stretching mode, C−H stretching mode in aromatic rings, O−H in-plane bending mode, and C−O stretching modes, all associated to phenolic groups. The band at 3282 cm^{-1} corresponds to O−H stretching mode of coupled carboxylic acids. In the region of C═O stretching modes, the superposition of two bands centered at 1685 cm^{-1} and 1651 cm^{-1} was observed, associated respectively to carboxylic acid and quinone groups.[47] The frequencies are somewhat lower than observed for free molecules, and this is characteristic of the coupling effect and formation of both inter- and intramolecular hydrogen bonds.[38] Quinone, phenol, and carboxylic acid groups, in decreasing order of content, were also distinguished in acid−base potentiometric titration studies for the SWNT-COOH sample. The first-order SWNT modes (C═C stretching modes) appeared as a doublet at 1544 and 1517 cm^{-1},[48] while, the low-intensity C−O bending modes were observed in the 900−1200 cm^{-1} spectral region.

The chemical modification of the SWNT-THIOP derivatives can be indicated in Figure 2b by several changes: (i) the appearance of thiophene stretching characteristic bands at 696 and 797 cm^{-1} due to out-of-plane C(2)−H stretching and asymmetric *cis* H−C(β)−C(β)H stretching of the thiophene ring, respectively; (ii) the appearance of C═C and C═S stretching modes of the thiophene ring; (iii) the very significant enhancement of the absorption associated with the C−O stretching mode between 1000 and 1200 cm^{-1}, characteristic of ester groups; (iv) the shift of the C═O stretching mode to higher frequencies (now at 1724 cm^{-1}), also characteristic of unsaturated or aryl esters; (v) the presence of bands around 2900 cm^{-1} and at ∼1440 cm^{-1} attributed respectively to symmetrical and asymmetrical C−H stretching and in-plane symmetrical bending vibrations in CH_2 groups.[47]Also, the presence of quinone groups is still evidenced by the C═O stretching mode of this group at ∼1676 cm^{-1}, but the bands initially associated to phenol and carboxylic acid groups have been removed. The results attest that the esterification reaction between the SWCNT-COOH and 2-(2-thienyl)ethanol has occurred in a good extension. As a secondary esterification reaction, the phenol groups could play the role of an alcoholic group and react with carboxylic acid groups to render lactones in intramolecular reactions or dimers in intermolecular reactions. The vibrational modes of lactone groups are in quite close frequencies to those of ester groups, but the very high intensity of the C−O stretching mode in the SWNT-THIOP spectrum shows the preferential occurrence of ester groups. Considering the complex environment of the chemically processed SWNT surface, intramolecular hydrogen bonds could also be responsible for the absence of characteristic phenolic vibrational bands, as occurring in the *o*-hydroxyacetophenone spectra.[47]

The UV−vis absorption spectra of the SWCNT, SWCNT-COOH, and SWCNT-THIOP composites with P3OT allowed the estimation of the optical gap as ∼1.8 eV for all the materials (Figure 1S of Supporting Information). No displacement of the absorption maximum was observed because of the presence of the carbon nanotube material. This implies that in the composite no significant ground state interaction is taking place between the carbon nanotube and the polymer, and hence no charge transfer occurs.[49] The fluorescence spectra, on the other hand (Figure 2S of Supporting Information), do show significant changes upon the addition of the carbon nanotubes. In fact, the fluorescence of the P3OT film is suppressed after adding 5 wt % of SWCNT (without purification) and SWCNT-THIOP. The fluorescence quenching was more effective for the film containing P3OT and pristine SWCNT, possibly because of the fact that the bound thiophene also acts as a nanotube-emitting chromophore, contributing to the emission in the P3OT/SWCNT-THIOP film. The fluorescence quenching may be attributed to suppression of singlet states in the P3OT due to an energy and/or charge-transfer process to the carbon nanotubes.[50] The appearance of a peak around 570 nm in the composites fluorescence spectra can be assigned to the carbon nanotube reflectance as also observed by Ago et al.[51]

Aiming to understand the nature of the polymer− SWCNT interaction, we carried out cyclic voltammetry measurements (Figure 3). In all cases we observed irreversible oxidation/reduction processes related to the formation of polarons/bipolarons in the poly(3-octylthiophene) chains. The addition of carbon nanotubes to the polymer matrix facilitates the polymer oxidation, as can be observed in Figure 3, leading to less positive values of oxidation potentials (1.19, 1.14, and 1.09 for P3OT, SWCNT-COOH + P3OT, and SWCNT-THIOP + P3OT, respectively). We attribute this effect to the interaction of the conducting polymer with a high density of π-electrons present at the carbon nanotube surface, promoting a decrease in the P3OT oxidation potential.[52] The largest decrease in oxidation potential was observed for P3OT/SWNT-THIOP, suggesting that, indeed, the presence of the thiophene groups linked to the nanotubes can be promoting a better dispersion of the SWCNT in the polymer matrix. It is important to point out that, as also observed in the absorption measurements, the polymer−carbon nanotube interaction in the ground state is poor, reflecting a difference of only 10 mV between the nonpurified and the SWCNT-THIOP composite. However, this small difference is enough to increase the reversibility of the oxidation/reduction processes in the P3OT/SWCNT-THIOP case, as a concomitant improvement of the definition of the

peaks. The latter indicates a reduction in the energetic disorder of the sites responsible for charge transport.

Atomic force microscopy (AFM) images of the pristine P3OT, P3OT/SWCNT, and P3OT/SWCNT-THIOP films were obtained in order to verify the effect of the addition of the SWCNT in the morphology of the composites. The rms roughness increases from pristine P3OT (2.8 nm) < P3OT/SWCNT-THIOP (3.6 nm) < P3OT/SWCNT (5.3 nm), indicating that the covalent modification gives a composite film with a much smoother surface in comparison to the nonmodified SWCNT composite film. The microstructure of all samples was found to be similar (Figure 4). However, both P3OT/SWCNT and P3OT/SWCNT-THIOP samples present large spatial period surface structures, represented by depressions and valleys in the images, possibly due to the presence of SWCNT bundles. However, in the modified-SWCNT composite film, the morphology is much more homogeneous, and the presence of these large period structures is much less evident. AFM studies reveal that even after chemical modification, the composite films still show evidence of SWNT bundles; however, the thiophene groups at the edges and defects, indeed, act coupling agents, improving the interaction between the two phases and providing a film morphology more similar to that of pristine P3OT.

Bulk Heterojunction SWCNT/Polymer Solar Cells. The characterization of the photovoltaic devices was made, determining the power conversion efficiency η quantitatively expressed by

$$\eta = \frac{V_{oc} J_{sc} \mathrm{FF}}{\Phi} \tag{1}$$

where Φ is the total irradiance, J_{sc} is the short-circuit current density, V_{oc} is the open circuit voltage, and FF is the fill-factor, which is given by

$$\mathrm{FF} = \frac{V_p I_p}{V_{oc} I_{sc}} \tag{2}$$

where V_p and I_p represent the maximum-power-rectangle of $I-V$, current−voltage, values.

Figure 5 shows the $I-V$ curves in the dark and under simulated AM 1.5 spectral distribution ($\Phi = 10.6$ W m^{-2}) for the P3OT+5 wt % of SWCNT (Figure 5a) and P3OT +5 wt % of SWCNT-THIOP (Figure 5b) solar cells in the forward bias region.

It is clearly evident that the introduction of blending levels of 5 wt % of SWCNT-THIOP into the P3OT polymer matrix increases both J_{sc} and V_{oc} in comparison to the solar cell assembled with the nonmodified SWCNT. J_{sc} and V_{oc} are equal to 9.5 μA cm^{-2} and 0.75 V, respectively, in the 5% blend device. Our results indicate that, indeed, the introduction of the pendant thiophene groups acts to enhance the interaction between the SWCNT and the P3OT. As a consequence, more polymer/nanotube internal junctions can be created through the film, increasing exciton dissociation and improving carrier transport. However, in accordance with the results observed by other groups, the short-circuit currents in the solar cells using carbon nanotubes are still low in comparison to other bulk heterojunctions devices. Causes for this can be ascribed mainly to the low charge carrier mobility in the P3OT matrix (10^{-4} to 10^{-6} cm^2 V^{-1} s^{-1}),[53] high recombination rate due to the low dispersion of the nanotubes, electrical shorting as the nanotubes penetrate the photoactive layer compromising the diode, and the presence of impurities.[15−19] Recently, Mitra and co-workers demonstrated the potential of SWCNT modification through the addition of C_{60}. The efficiency obtained is one of the highest reported so far, 0.5% at 95 mW cm^{-2}. The C_{60} is expected to increase the exciton dissociation while the SWCNTs improve the electron transport.[54]

The reason for the low V_{oc} observed in our 5 wt % SWCNT + P3OT solar cell in comparison to the values reported by other groups,[13,18] who show values higher than 0.6 V, may be attributed to different contents of SWCNT dispersed in the polymer (5 wt % in our case), different sources of carbon nanotubes and purification processes, different proportions of metallic nanotubes, the degree of aggregation, and the level of impurities, among others. As a consequence, the broad range of results obtained by different groups makes a direct comparison difficult. Grobert, in a recent review, comments how the preparation and purification steps developed by different labs can produce nanotubes with diverse electronic properties, without mention that the information provided by the companies are far from what is, in fact, found in the samples.[55] The achievement of high purity SWCNT free of defects and with controlled amounts of metallic and semiconducting species is a challenge pursued by the groups working with these materials.

Optimization of the SWCNT concentration for maximum current density is a necessary step in order to improve the overall efficiency of the solar cells. Characterization of the single layer polymer solar cells showed a corresponding increase in the J_{sc} and V_{oc} as the concentration of SWCNT-THIOP increases in the P3OT matrix. Figure 6 shows the $I-V$ curves under simulated AM 1.5 illumination for the P3OT+SWCNT-THIOP cells, at different modified SWCNT concentrations.

As the concentration varies from 1 to 5 wt % of SWCNT-THIOP in the P3OT polymer, both J_{sc} and V_{oc} increase as consequences of better carrier separation and transport upon addition of the acceptor material, as discussed previously. However, for the cell with 7 wt % of SWCNT-THIOP, a drastic reduction in the performance is observed. This effect may be a consequence of the increase in the content of metallic tubes, short-circuiting the cell at high concentration and reducing the shunt resistance. However, the possibility that in this sample the concentration limit for homogeneous distribution of carbon nanotube terminations has been exceeded cannot be excluded. At concentrations higher than this limit, phase segregation would be expected to promote SWCNT aggregation, reducing exciton dissociation efficiency.

The increase of J_{sc} with increasing SWCNT content occurs until a critical concentration is achieved, since a larger amount of SWCNT results in a higher concentration of exciton dissociation sites and better transport for charge carriers. The concomitant increase of V_{oc}, however, is intriguing. It suggests that higher SWCNT concentrations below the critical limit tend to reduce the short occurrence, increasing the shunt resistance. Presently, however, we have neither additional experimental data supporting this hypothesis nor a description of the working mechanism to propose, so that further experimental work will certainly be necessary to clarify this point.

Conclusions

In this work we have demonstrated that chemical modification on carbon nanotube edges and defects by the introduction of pendant thiophene groups is an interesting route for polymer solar cells using SWCNT. Similar to other applications using carbon nanotubes, photovoltaic devices also require a good dispersion of these materials. The chemical functionalization presented here allowed the preparation of polymer composites with improved compatibility between the polymer and the

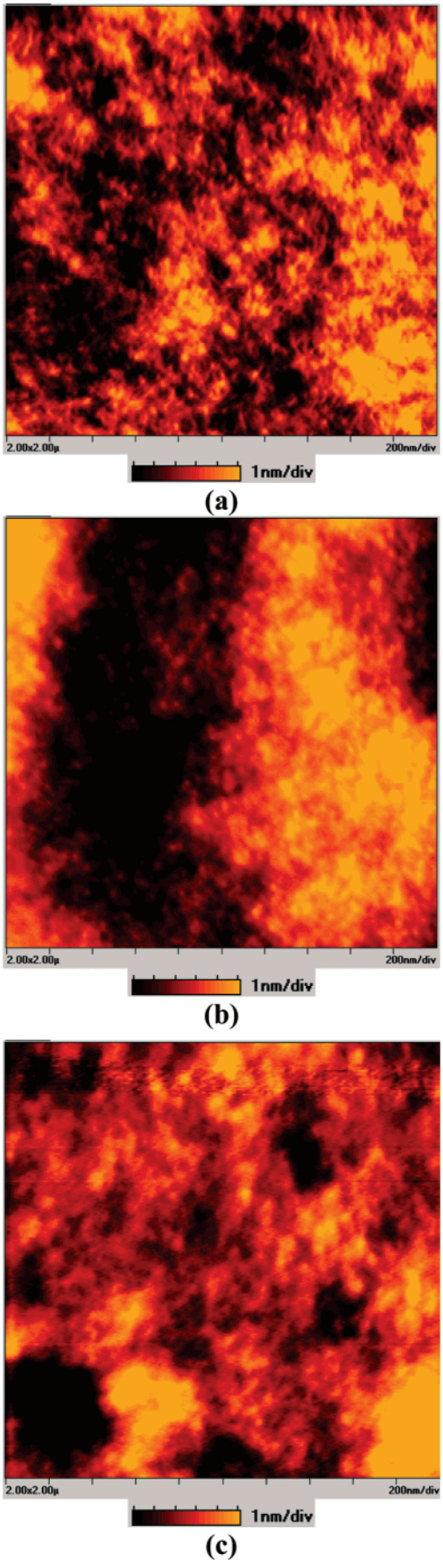

Figure 4. AFM images of a pristine P3OT (a), P3OT + 5 wt % of SWCNT (b), and P3OT + 5 wt % of SWCNT-THIOP (c) film spin-coated on mica substrate from chloroform solution.

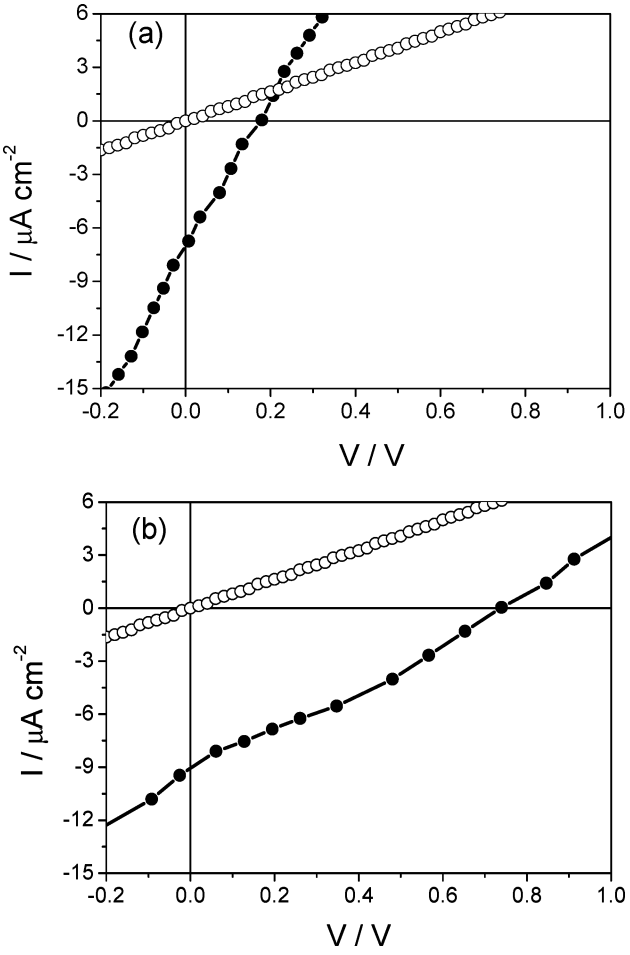

Figure 5. (a) $I-V$ characteristics of an ITO/PEDOT:PSS/SWCNT (5 wt %) + P3OT/Al device in the dark (open circles) and under illumination (filled circles, AM 1.5, 10.6 W m^{-2}). (b) The same data for an ITO/PEDOT:PSS/SWCNT-THIOP (5 wt %) + P3OT/Al device.

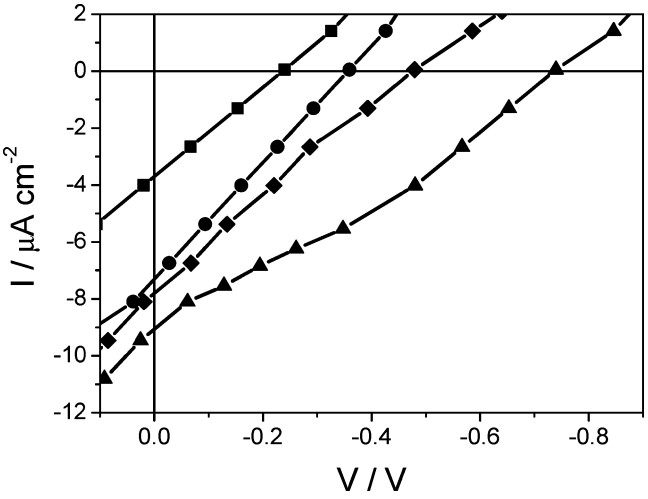

Figure 6. $I-V$ characteristics under simulated AM 1.5 illumination ($\Phi = 10.6$ W m^{-2}) for the polymer solar cells using P3OT composites with different SWCNT-THIOP doping levels. The device configuration is the same as described in Figure 4: (■) 1 wt %; (●) 3 wt %; (▲) 5 wt %; (◆) 7 wt %.

SWCNT phases as demonstrated by spectroscopic, electrochemical, and microscopic investigations. In our work, the solar cells using the modified SWCNT with thiophene groups showed better performance in comparison to the polymer cell assembled with pristine SWCNT. Increasing the dopant level up to 5 wt

% of SWCNT-THIOP has contributed positively to increase both J_{sc} and V_{oc}. Above this concentration, the performance is drastically reduced, possibly due the introduction of short-circuits from the metallic nanotube components and reduction of the effectiveness of the exciton dissociation process. The reason for not observing a drastic increase in device performance in comparison to literature may be related to the fact that even after chemical modification, the major part of the nanotubes is still present in form of bundle, although in a smaller extension than that of the samples containing nonmodified nanotubes.

In summary our results indicate that the anchoring thiophene groups act as a coupling agent, improving interaction between polymer and nanotube phases. This improved morphology is responsible for the increase in both exciton splitting and charge carrier transport. Further improvements in device performance, especially in the fill factor and short-circuit current, are expected with more controlled film preparation (different solvents, deposition, and annealing) and separation of the semiconducting from the metallic nanotubes.

Acknowledgment. The authors thank the Brazilian agencies FAPESP, CAPES, FAPEMIG, and CNPQ, the networks Carbon Nanotube Research, IM^{2}C, and RENAMI for research grants, Dr. Ryan C.White for English revision, G. Conturbia and R. L. Patyk for sample and device preparation assistance, and J. Hermes and M. Cotta (Physics Institute, Unicamp) for AFM analysis and discussions.

Supporting Information Available: Absorption spectra of the carbon nanotube composite films; luminescence spectra of the pristine P3OT and composite films, HR-TEM of the pristine nanotube after HNO_3 treatment. This material is available free of charge via the Internet at http://pubs.acs.org.

References and Notes

(1) Dresselhaus, M. S.; Dresselhaus, G.; Avouris, P. *Carbon Nanotubes: Synthesis, Structure, Properties and Applications*; Springer: Berlin, Germany, 2001.

(2) Dresselhaus, M. S.; Lin, Y. M.; Rabin, O.; Jorio, A.; Souza, Filho, A. G.; Pimenta, M. A.; Saito, R.; Samsonidze, G. G.; Dresselhaus, G. *Mater. Sci. Eng. C* **2003**, *23*, 129.

(3) Haddon, R. C. *Acc. Chem. Res.* **2002**, *35*, 997.

(4) Bryning, M. B.; Islam, M. F.; Kikkawa, J. M.; Yodh, A. G. *Adv. Mater.* **2005**, *17*, 1186.

(5) Javea, A.; Guo, J.; Wang, Q.; Lundstrom, M.; Dai, H. J. *Nature.* **2003**, *424*, 654.

(6) Sariciftci, N. S.; Smilowitz, L.; Hegeer, A. J.; Wudl, F. *Science.* **1992**, *258*, 1474.

(7) Halls, J. J. M.; Walsh, C. A.; Greenham, N. C.; Marseglia, E. A.; Friend, R. H.; Moratti, S. C.; Holmes, A. B. *Nature* **1995**, *376*, 498.

(8) Li, G.; Shrotriya, V.; Huang, J.; Yao, Y.; Moriarty, T.; Emery, K.; Yang, Y. *Nat. Mater.* **2005**, *4*, 864.

(9) Brabec, C. J.; Sariciftci, N. S.; Hummelen, J. C. *Adv. Funct. Mater.* **2001**, *11*, 15.

(10) Li, N.; Huang, Y.; Du, F.; He, X.; Lin, X.; Gao, H.; Ma, Y.; Li, F.; Chen, Y.; Eklund, P. C. *Nano Lett.* **2006**, *6*, 1141.

(11) Sandler, J. K. W.; Kirk, J. E.; Kinloch, I. A.; Shaffer, M. S. P.; Windle, A. H. *Polymer.* **2003**, *44*, 5893.

(12) Ago, H.; Shaffer, M. S. P.; Ginger, D. S.; Windle, A. H.; Friend, R. H. *Phys. Rev. B* **2000**, *61*, 2286.

(13) Landi, B. J.; Rafaelle, R. P.; Castro, S. L.; Bailey, S. G. *Prog. Photovolt.: Res. Appl.* **2005**, *13*, 165.

(14) Bhattacharyya, S.; Kymakis, E.; Amaratunga, G. A. J. *Chem. Mater.* **2004**, *16*, 4819.

(15) Kymakis, E.; Alexandrou, I.; Amaratunga, G. A. J. *J. Appl. Phys.* **2003**, *93*, 1764.

(16) Kymakis, E.; Amaratunga, G. A. J. *Solar Energy Mater. Solar Cells* **2003**, *80*, 465.

(17) Canestraro, C. D.; Schnitzler, M. C.; Zarbin, A. J. G.; da Luz, M. G. E.; Roman, L. S. *Appl. Surface Sci.* **2006**, *252*, 5575.

(18) Barazzouk, S.; Hotchandani, S.; Vinodgopal, K.; Kamat, P. V. *J. Phys. Chem. B* **2004**, *108*, 17015.

(19) Kymakis, E.; Amaratunga, G. A. J. *Appl. Phys. Lett.* **2002**, *80*, 112.

(20) Kymakis, E.; Amaratunga, G. A. J. *Adv. Mater Sci.* **2005**, *10*, 300.

(21) Kymakis, E.; Koudoumas, E.; Franghiadakis, I.; Aramatunga, G. A. J. *J. Phys. D: Appl. Phys.* **2006**, *39*, 1058.

(22) Hasobe, T.; Fukuzumi, S.; Kamat, P. V. *J. Phys. Chem. B* **2006**, *110*, 25477.

(23) Sgobba, V.; Aminur, Rahman, G. M.; Guldi, D. M.; Jux, N.; Campidelli, S.; Prato, M. *Adv. Mater.* **2006**, *18*, 2264.

(24) Castrucci, C.; Tombolini, F.; Scarselli, M.; Speiser, E.; Del, Gobbo, S.; Ritcher, W.; De Crescenzi, M.; Diociaiutti, M.; Gatto, E.; Venanzi, M. *Appl. Phys. Lett.* **2006**, *89*, 253107.

(25) Baskaran, D.; Mays, J. W.; Zhang, X. P.; Bratcher, M. S. *J. Am. Chem. Soc.* **2005**, *127*, 6916.

(26) Guldi, M. D.; Rahman, G. M. A.; Zerbetto, F.; Prato, M. *Acc. Chem. Res.* **2005**, *38*, 871.

(27) Guldi, M. D.; Rahman, G. M. A.; Jux, N.; Tagmatarchis, N.; Prato, M. *Angew. Chem., Int. Ed.* **2004**, *43*, 5526.

(28) Guldi, M. D.; Rahman, G. M. A.; Prato, M.; Jux, N.; Qin, S.; Ford, W. *Angew. Chem., Int. Ed.* **2005**, *44*, 2015.

(29) Alvaro, M.; Atienzar, P.; De la Cruz, P.; Delgado, J. L.; Troiani, V.; Garcia, H.; Langa, F.; Palkar, A.; Echegoyen, L. *J. Am. Chem. Soc.* **2006**, *128*, 6626.

(30) Ballesteros, B.; de la Torre, G.; Ehli, C.; Aminur, G. M.; Agullo-Rueda, F.; Guldi, D. M.; Torres, T. *J. Am. Chem. Soc.* **2007**, *129*, 5061.

(31) Cioffi, C.; Campidelli, S.; Sooambar, C.; Marcaccio, M.; Marcolongo, G.; Meneghetti, M.; Paolucci, D.; Paolucci, F.; Ehli, C.; Aminur, G. M.; Sgobba, V.; Guldi, D. M.; Prato, M. *J. Am. Chem. Soc.* **2007**, *129*, 3938.

(32) Rowell, M. W.; Topinka, M. A.; McGehee, M. D.; Prall, H.-J.; Denler, G.; Sariciftci, N. S.; Hu, L.; Gruner, G. *Appl. Phys. Lett.* **2006**, *88*, 233506.

(33) Van, de Lagemaat, J.; Barnes, T. M.; Rumbles, G.; Weeks, C.; Levitsky, I.; Peltola, J.; Glatkowski, P. *Appl. Phys. Lett.* **2006**, *88*, 233503.

(34) Li, J.; Hu, L.; Zhou, Y.; Wang, L.; Grüner, G.; Marks, T. J. *Nano Lett.* **2006**, *6*, 2472.

(35) Saran, N.; Parikh, K.; Suh, D-S.; Muñoz, E.; Kolla, H.; Manohar, S K. *J. Am. Chem. Soc.* **2004**, *126*, 4462.

(36) Jansseune, T. *Comp. Semicond.* **2005**, *11*, 34.

(37) Patyk, R. L.; Lomba, B. S.; Nogueira, A. F.; Furtado, C. A.; Santos, A. P.; Mello, R. M. Q.; Micaroni, L.; Hümmelgen, I. A. *Phys. Status Solidi* **2007**, *1*, 43.

(38) Sugimoto, R.; Takeda, S.; Gu, H. B.; Yoshini, K. *Chem. Express* **1986**, *1*, 635.

(39) Kim, U. J.; Furtado, C. A.; Liu, X. M.; Chen, G.; Eklund, P. C. *J. Am. Chem. Soc.* **2005**, *127*, 15437.

(40) Alvaro, M.; Atienzar, P.; De la Cruz, P.; Delgado, J. L.; Garcia, H.; Langa, F. *Chem. Phys. Lett.* **2004**, *386*, 342.

(41) Vieira, H. S.; Andrada, D. M.; Martins, M. D.; Macedo, W. A. A A.; Santos, P.; Pimenta, L. A.; Gorgulho, H. F.; Moreira, R. L.; Jorio, A.; Pimenta, M. A.; Furtado, C. A. *J. Nanosci. Nanotechnol.*, in press.

(42) Jorio, A.; Saito, R.; Hafner, J. H.; Lieber, C. M.; Hunter, M.; McClure, T.; Dresselhaus, G.; Dresselhaus. M. S. *Phys. Rev. Lett.* **2001**, *86*, 1118.

(43) Pimenta, M. A.; Marucci, A.; Empedocles, S.; Bawendi, M.; Hanlon, E. B.; Rao, A. M.; Eklund, P. C.; Smalley, R. E.; Dresselhaus, G.; Dresselhaus, M. S. *Phys. Rev. B* **1998**, *58*, R16016.

(44) Brown, S. D. M.; Jorio, A.; Corio, P.; Dresselhaus, M. S.; Dresselhaus, G.; Saito, R.; Kneipp, K. *Phys. Rev. B* **2001**, *63*, 155024.

(45) Rao, A. M.; Eklund, P. C.; Bandow, S.; Thess, A.; Smalley, R. E. *Nature* **1997**, *388*, 257.

(46) Knight, D. S.; Pântano, C. G.; White, W. B. *J. Mater. Res.* **1989**, *4*, 385.

(47) Silverstein, R. M.; Webster, F. X. *Spectrometric Identification of Organic Compounds*; John Wiley & Sons: New York, 1998; Chapter 3.

(48) Kim, U. J.; Liu, X.; Furtado, C. A.; Gugang, C.; Gutierrez, H. R.; Saito, R.; Jiang, J.; Dresselhaus, M. S.; Eklund, P. C. *Phys. Rev. Lett.* **2005**, *95*, 15740.

(49) Kymakis, E.; Amaratunga, G. A. J. *Synth. Met.* **2004**, *142*, 161.

(50) Chirvase, D.; Chiguvare, Z.; Knipper, M.; Parisi, J.; Dyakonov, V.; Hummelen, J. C. *J. Appl. Phys.* **2003**, *93*, 3326.

(51) Ago, H.; Petrisch, K.; Shaffer, M. S. P.; Windle, A. L.; Friend, R. H. *Adv. Mater.* **1999**, *11*, 1281.

(52) Bavastrello, V.; Carrara, S.; Kumar, Ram, M.; Nicolini, C. *Langmuir* **2004**, *20*, 969.

(53) Valaski, R. L.; Moreira, M.; Micaroni, L.; Hümmelgen, I. A. *Braz. J. Phys.* **2003**, *33*, 392.

(54) Li. C.; Chen, Y.; Iqbal, Z.; Chhowalla, M.; Mitra, S. *J. Mater. Chem.* **2007**, *17*, 2406.

(55) Grobert, N. *Mater. Today* **2007**, *10*, 28.